Published by
NIGERIAN SOCIETY OF PHYSICAL SCIENCES
Available online @ https://journal.nsps.org.ng/index.php/jnsps

J. Nig. Soc. Phys. Sci. 4 (2022) 892

Journal of the Nigerian Society of Physical Sciences

Effect of temperature on optical, structural, morphological and antibacterial properties of biosynthesized ZnO nanoparticles

G. Kamarajan[a], D. Benny Anburaj[a,*], V. Porkalai[b], A. Muthuvel[c], G. Nedunchezhian[d]

[a] *PG and Research Department of Physics, D.G. Government Arts College (Affiliated to Bharathidasan University, Trichy), Mayiladuthurai, Tamil Nadu-609001, India.*
[b] *Nethaji Subash Chandra Bose College for Co-ed (Affiliated to Bharathidasan University, Trichy), Senthemangalam, Thiruvarur, Tamilnadu-614001, India.*
[c] *PG and Research Department of Physics, T.B.M.L. College (Affiliated to Bharathidasan University, Trichy), Porayar, Tamil Nadu-609307, India.*
[d] *PG and Research Department of Physics, Thiru. Vi. Ka. Government Arts College (Affiliated to Bharathidasan University, Trichy), Thiruvarur, Tamil Nadu-61003, India.*

Abstract

Nanomaterials can be produced by using nontoxic biological compounds that are both eco-friendly and economically viable. Temperature dependent ecological synthesis of ZnO nanoparticles was carried out with leaf extract of *Ocimum sanctum*. An electron microscope study confirmed that a temperature of 400 $^{\circ}C$ was optimal for the formation of ZnO nanoparticles generated by biosynthesizing ZnO nanoparticles. The normal crystalline size of biosynthesized ZnO nanoparticles calculated via XRD analysis are found to be 18, 12 and 17 nm for 300 – 500 $^{\circ}C$, respectively. The direct optical band gap energy deducted from Tauc approximation range to be 3.32-3.20 eV. In SEM analysis, depending on the temperature of the synthesis conditions, different ZnO morphologies are also found. Functional groups analysis confirmed the incidence of carboxyl and amide groups in the *O. sanctum* leaf extract. The ZnO nanoparticles analysed at room temperature using photoluminescence, a broad visible band is observed around 382 nm for all samples. Furthermore, this study determines that the synthesized ZnO nanoparticles provide antimicrobial efficacy against clinical strains of *Bacillus subtilis* and *Staphylococcus aureus*, as well as against standard strains of *Escherichia coli*. Several fields, including cosmetics and pharmaceuticals, can benefit from biosynthesized nanoparticles.

DOI:10.46481/jnsps.2022.892

Keywords: Nanoparticles, *Ocimum sanctum*, ZnO, SEM, DLS, Antibacterial.

Article History :
Received: 26 June 2022
Received in revised form: 14 July 2022
Accepted for publication: 15 July 2022
Published: 20 August 2022

Communicated by: K. Sakthipandi

1. Introduction

Nanotechnology is causing a revolution in every discipline of science by incorporating nanoparticles into diverse industrial and medical products such as ceramic materials, cosmetics, food and pharmaceuticals [1]. Due to their extraordinary properties such as nanoparticles insignificant size, high adsorption, high catalytic activity, high surface area, large number reactive sites and chemical stability, nanoparticles are a promising strategy to improve medical and industrial applications [2]. Nanoparticles, e.g., ZnO, CuO, CaO, SiO_2 , MgO and TiO_2, have received significant scientific attention due to their potential applications as biocidal agents and disinfectants, especially in the healthcare field [3-8]. Due to

*Corresponding author tel. no:
Email address: bennyanburaj@gmail.com (D. Benny Anburaj)

their high stability, ZnO nanoparticles are considered probable next-generation constituents as biocidal and disinfecting agents. This stability is ascribed to them being more versatile than organic-based sanitizers and anti-microbial mediators [9]. As a semiconductor, ZnO has a wideband gap (3.37 eV) and an exciton binding energy of 60 meV, which is an efficient source of excitonic blue radiation. As a result of its inherent ability to absorb UV irradiation, ZnO has been agreed by the nutrition and drug management for use in sunscreens [10]. ZnO nanoparticles have been by many methods including Sol gel [3], chemical vapor deposition [11], chemical precipitation [12], hydrothermal [13], laser ablation [14] and pyrolysis [15]. This process is complicated, costly and results in hazardous toxic wastes that are harmful to humans and the environment. These methods are also limited in biomedical application because of the toxic chemicals required [9]. Hence, it is imperative to explore alternative green source in order to overcome these disadvantages. Various natural sources have been used in the green synthesis process, including plants, bacteria, algae and fungi [16]. Biosynthesized nanoparticles are biocompatible, eco-friendly and non-toxic [9]. The natural extract may contain bioactive compounds that are likely to bind to nanoparticles surface, and the density of their population depends on the synthesis parameters [17]. Phytochemicals, such as amino acids, flavones, phenols, sugars, carotenes, aldehydes, amides, ketones, etc., present in plants have been widely used for green synthesis. The surface coatings of the fabricated materials are controlled by the interaction between nanoparticles and biological materials [3]. There have been numerous reports on the combination of ZnO nanoparticles with leaf extracts, such as *Azadirachta indica* [18], *Solanum nigrum* [3], *Passiflora caerulea* [19] *Moringa oleifers* [20], *Cinnamomum verum* [21], *Curry* [9], and their antimicrobial activities.

Ayurveda and its allied herbalism disciplines are integral parts of Indian traditional medicine. *Ocimum sanctum* (*O. sanctum*) has been used for its diverse medicinal properties for thousands of years. The *O. sanctum* has been shown to possess antibacterial, anti- inflammatory, antistress, antiasthmatic, immunomodulatory and hypoglycemic properties in various animal models [22]. It relieves stress and improves immunity, as well as relieving people of stress. Alkaloids, carvacrol, ursolic, tannins, linalool, Rosmarinus acid, glycosides are among the chemical constituents of *O. sanctum*. We synthesized ZnO nanoparticles using *O. sanctum* leaf extract at changed calcinations temperatures in the current study. The biosynthesized nanoparticles were characterized by Scanning electron microscopy (SEM) with energy dispersive X-ray spectroscopy (EDAX), Zeta potential (ZE), UV-visible spectroscopy (UV-vis), Dynamic light scattering (DLS), X-ray diffraction analysis (XRD), Fourier transform infrared spectroscopy (FT-IR) and Photoluminescent (PL) analysis. Furthermore, the stability of the different calcinations' temperature ZnO nanoparticles and their antibacterial activity were also studied.

2. Experimental sections

2.1. Materials

The substances such as Zinc acetate dihydrate (Zn $(CH_3COO)_2.2H_2O$) and all the chemicals and reagents were procured since Merck chemical reagent co distilled this work purchased since the leaves of *O*. Sanctum plant together form in and around garden, Nagapattinam, Tamil Nadu, India.

2.2. Plant leaf collection

Fresh leaves of plants that is, *O. sanctum* free as of were collected from Nagapattinam. The leaves were recognized and authentic by Department of Agriculture, Annamalai University at Tamil Nadu. To remove dust particles from the surface of the leaves, they were twice washed by tap water and then repeatedly washed in double distilled water. The washed leaves then shade dried for five days. Before, 20 gm of dried leaves be situated crushed and 50 ml of distilled water were added. Subsequently that, a magnetic stirrer was used to stir the mixture, then the mixture was heated for 60 $^{\circ}C$ at 1 h. After the combination displayed a creamy (yellow) color, it was sifted with Whatman filter paper. As a result, nanoparticles of ZnO were prepared from the extract solution.

2.3. Preparation of ZnO nanopowders

The ZnO nanoparticles were biosynthesized by following the Sol gel method designated by Muthuvel et al. [3]. Briefly, it was prepared by stirring 2 M zinc acerate in 50 mL of deionized water for 30 min at 85 $^{\circ}C$. on order to make a NaOH solution, 4 gm NaOH powder was additional to 50 mL of distilled water and stirred concurrently at 85 $^{\circ}C$ for 30 min. The two solutions were then vigorously stirred together. The 15 mL leaf extract was assorted through the solution drop by drop during this stirring process. After stirring continuously for two 2 h using a magnetic stirrer white precipitate was obtained. To remove the impurities, the hurried was filtered and repeatedly washed with distilled water followed by ethanol. After, the precipitate was dried at 300 $^{\circ}C$ for 4 h and the obtained ZnO powder was endangered for additional classification. The similar procedure followed by other two temperature (400 $^{\circ}C$ and 500 $^{\circ}C$).

2.4. Characterization of synthesized nanoparticles

In order to collect X-ray diffraction data for the formed samples, SHIMADZU-XRD 6000 analytical diffractometers were used. We measure UV absorbance and photoluminescence with a Shimadzu UV-VIS-260 system. The morphology of the synthesized nanoparticles was examined using scanning electron microscopy (Hitachi S-4500 machine). DLS and zeta potential were measured by Malvern Zeta Sizer (ZS 90, USA). Measurements were made with a Bruker tensor 27 FT-IR spectrometer using Fourier transform infrared spectra.

2.5. Antibacterial activities

The antibacterial actions of leaf extract and biosynthesized ZnO nanoparticles (400 °C) were tested with the Disc diffusion technique [23] on IV types of bacteria: *Bacillus subtilis*, *Staphylococcus aureus*, Pseudomonas aeruginosa and *Escherichia coli*. The samples of 5 and 10 μg/mL concentration were dispensed onto ach disk and positioned on Muller Hinton agar plates. The antibiotic dis Ciprofloxacin was used as positive controller. The plates were gestated for 24 h at 35 °C. The antibacterial activities of the samples on the tested bacterial strains were determined by forming an inhibitory zone around the wells.

3. Results and analysis

3.1. XRD analysis

Figure 1 shows the XRD patterns of the biosynthesised ZnO nanoparticles prepared at 300 °C, 400 °C, and 500 °C. All the peaks with Miller indices (100), (022), (101), (102), (110), (103) and (200) are detectable in that ZnO nanoparticles which were calcined at three different temperatures respectively. ZnO nanoparticles were scheduled as a hexagonal Wurtzite structure in all the diffraction pattens. The similar results were also reported by others the (h k I) standards are settled well with the standard card of ZnO powder model [JCPDS file No: 89-7102] [24].

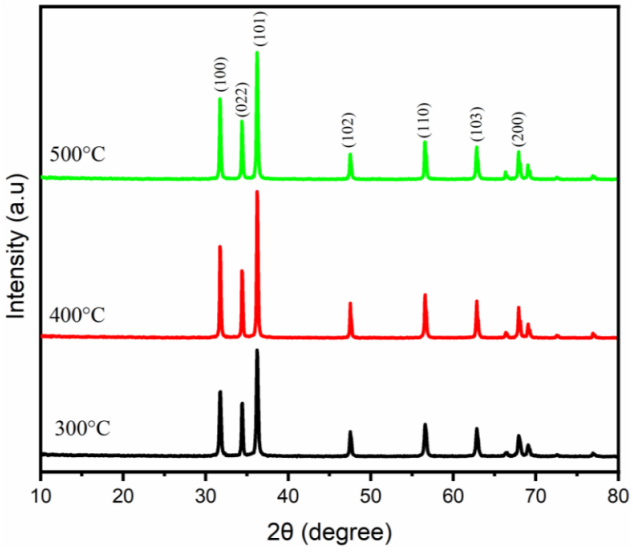

Figure 1: XRD pattern of the biosynthesized ZnO nanoparticles calcined at three different temperatures

A single phase ZnO nanoparticles was synthesized based on the results, and no additional peaks were detected. In this case, the extensive peaks suggest the crystalline size particles are at the nanoscale, indicating the size of the biosynthesized particles is well and insignificant [24]. As a result, ZnO nanoparticles synthesized at 400 °C contain all the characteristic diffraction peaks that show the nanoparticles are crystalline in nature. For all investigated annealing temperatures, (101) has the strongest line (Figure 1.) The result of this study indicate that the method used to make pure ZnO nanoparticles is effective. From the figure also shows that the diffraction peak intensifies and narrows as the annealing temperature increases, suggesting that the product of crystallizing ZnO nanoparticles has a good crystalline structure.

Furthermore, the broadening at the bottom of the diffraction peaks in Figure 1 indicates that ZnO nanoparticles crystalline sizes are small which consistent with ZnO nanoparticles sizes reported in literature [25]. Through a rise in the annealing temperature from 400 °C to 500 °C, the crystallinity of the ZnO nanoparticles improves, as shown in Figure 1. The Scherer method was used to estimate the size of the synthesized nanoparticles [26]:

$$D = \frac{0.89\ \lambda}{\beta \cos\theta} \tag{1}$$

where D is particle size of the crystal, $k = 0.9$ is Scherer's constant, λ is X-ray wavelength (1.5406Å), β is the width of the XRD peak at the half height and θ is Bragg's diffraction angle. The micro-strain (ϵ) and dislocation density δ were considered using the formulas [26]:

$$\epsilon = \frac{\beta \cos\theta}{4} \tag{2}$$

$$\delta = \frac{1}{D^2} \tag{3}$$

The changes in calcinate temperature led to changes in crystallite size, as shown in Table 1. From the increasing sintering temperature temperatures up to 400 °C, the size of the average crystallite increases. As result, ZnO nanoparticles are observed to have a quantity of vacancies of oxygen situation bands and lattice defects at the boundary, causing the unit cell volume to decrease. Although it can relax the interface structure of ZnO nanoparticles at low temperature (300 °C), it cannot eradicate the resident lattice disorder or variation their internal structure [3, 9]. The sintering occurs at 400 °C, which causes the lattice parameters to adjust rapidly, and the unit cell volume to normalize as the modicums initiate to grow [18]. In addition to the increase in crystal size at sophisticated sintering temperature (500 °C), large scale particles also develop during sintering due to the organization of minor grains by grain borderline dispersion. The present study demonstrates that ZnO nanoparticles obtained by biosynthesis can greatly improve antibacterial activity when they are deriving from a smaller crystal size (12 nm).

3.2. UV-Visible analysis

Using a double beam UV-Vis spectrophotometer, we recorded the absorption spectra of biosynthesized ZnO nanoparticles. In the range of 200-800 nm, the samples absorption spectrum was recorded. Figure 2a shows the biosynthesized ZnO nanoparticles at different calcinated temperature. The biosynthesized ZnO nanoparticles presented absorption edges at 373, 387 and 379 nm at 300 °C, 400 °C and 500 °C,

Table 1: Structural parameters of biosynthesized ZnO nanoparticles at different calcinations temperature

Sample	Calcination temperature	Grain size (D nm)	Dislocation density (10^{15} (lines/m^2))	Strain ($\epsilon \times 10^{-3}$)	Lattice parameter (Å)			Volume (Å^3) (10^3)
					A	c	c/a	
ZnO	300 °C	18	0.4527	10.1173	2.8671	4.959	1.72933	35.32
ZnO	400 °C	12	1.1111	7.4687	2.86227	4.957	1.73184	35.16
ZnO	500 °C	17	6.9444	6.1173	2.77382	4.954	1.78670	33.33

respectively. A strong absorption peak was observed in all synthesized nanoparticles in the UV-visible region. At 400 °C, the absorption spectrum showed a red shift due to a qualitative suggestion of the crystal size distribution.

We calculated the band gap energy (E_g) of biosynthesized ZnO nanoparticles based on the wavelength value associated with the connection theme of the vertical and horizontal parts of the band [3]:

$$(\alpha h\nu)^2 = B\left(h\nu - E_g\right)^{1/2}, \tag{4}$$

where h is the Planck constant, $h\nu$ is photon energy, α is the absorption factor and B is a constant. The optical band gap of biosynthesized ZnO nanoparticles synthesized at 300 °C, 400 °C and 500 °C, respectively, is calculated to be 3.32, 3.20 and 3.27 eV, respectively (figure 2b). With increasing sintering temperatures, the optical band gap energy decreases. In comparison with bulk ZnO nanoparticles (E_g = 3.35 eV), the band gap value decreases, indicating the quantum confinement effect [26]. The present optical band gap energy (E_g = 3.2 eV) is very low to the ZnO nanoparticles synthesized by some chemical methods [27, 28]. The present work demonstrates that ZnO nanoparticles can be obtained by biological means from small band gap values, and that this greatly enhances their antibacterial properties.

3.3. Dynamic light scattering and zeta potential analysis

By measuring the time dependent instability of scattering of light by nanoparticles enduring Brownian movement, the particle size spreading was resolute using dynamic light scattering analysis [23]. In colloidal solution, dynamic light scattering is widely used to quantity the explosive thickness of capping agents or stabilizers invasive metallic nanoparticles, as well as the size of the metallic core. Figure 3a shows the DLS pattern of biosynthesized ZnO nanoparticles at different calcinated temperature. The size distribution of biosynthesized ZnO nanoparticles at 300 °C, 400 °C and 500 °C, respectively, is 47, 32 and 50 nm. According to the DLS data, variations in nanoparticles size can be attributed to temperature variations [3].

The zeta potential values provide information regarding a samples surface area charge as well as its stability. Figure 3b shows that ZnO nanoparticles biosynthesized at 300 °C, 400 °C and 500 °C, have zeta potentials of -24.86, -26.48 and -23.19 mV, respectively (figure 3b). There are similar kinds of results reported by Muthuvel et al [3]. Particles through ZE above +30 mV or below −30 mV are considered constant. With a zeta potential of −26.48 mV, the ZnO nanoparticles synthesized via biosynthesis at 400 °C are very stable. The high negative value of the zeta potential correlated with the presence of negatively charged groups on the superficial of the nanoparticles. This reduction of metal ions also stabilization of nanoparticles could be caused by protein and flavonoids in the leaf extract [18].

3.4. SEM analysis

Using SEM microscopy, the ZnO nanoparticles were considered for their form and size. Figure 4 displays the SEM images of biosynthesized ZnO nanoparticles at three calcined temperatures. All the samples have spherical shapes and nanosized rings. At lower temperatures, nanoparticles were more clumped; on increasing the temperature, segregation was observed, and at the highest temperature, the most segregation of nanoparticles was evident, and individual nanoparticles were more visible. For biosynthesized ZnO nanoparticles, the even surface morphology besides modicum size is measured by 400 °C. Biosynthesized of ZnO nanoparticles induced added unvarying structure and hexagonal also clear nanoparticles structure at 400 °C (figure 4, a3). The histogram of particle size distribution in figure 4 (b1-b3) shows the average diameter of ZnO nanoparticles as 36, 30 and 31 nm for 300 °C, 400 °C and 500 °C, respectively.

EDAX analysis of biosynthesized ZnO nanoparticles at different calcined temperatures; Znic and oxygen confirms the presence of metallic zinc acetate during the biosynthesis of ZnO nanoparticles. Zinc and oxygen are each represented by two peaks in the EDAX spectrum (Figure 5). The EDAX analysis revealed that as the temperature increased, the more ZnO nanoparticles were formed. It can be seen from the graph that at lower temperature 72.1 of zinc was analysed, whereas at 400 °C this number increased to 78.2 %. Oxygen in trace amounts is a reflection of plant phytochemicals reducing metal ions, acting as capping agents, and stabilizing the biosynthesis of ZnO nanoparticles [9]. In biosynthesis ZnO nanoparticles using leaf extract, the EDAX profile showed higher counts at 10keV due to zinc oxide ions, which confirmed the formation of ZnO nanoparticles.

3.5. FT-IR analysis

FT-IR investigation can be used to classify the probable reducing and stabilizing bio molecules. Wave number range between 400 to 4000 cm^{-1} was used for FT-IR analysis. Figure 6 shows the FT-IR spectra of the synthesized ZnO nanoparticles at different calcined temperature. The FT-IR spectrum

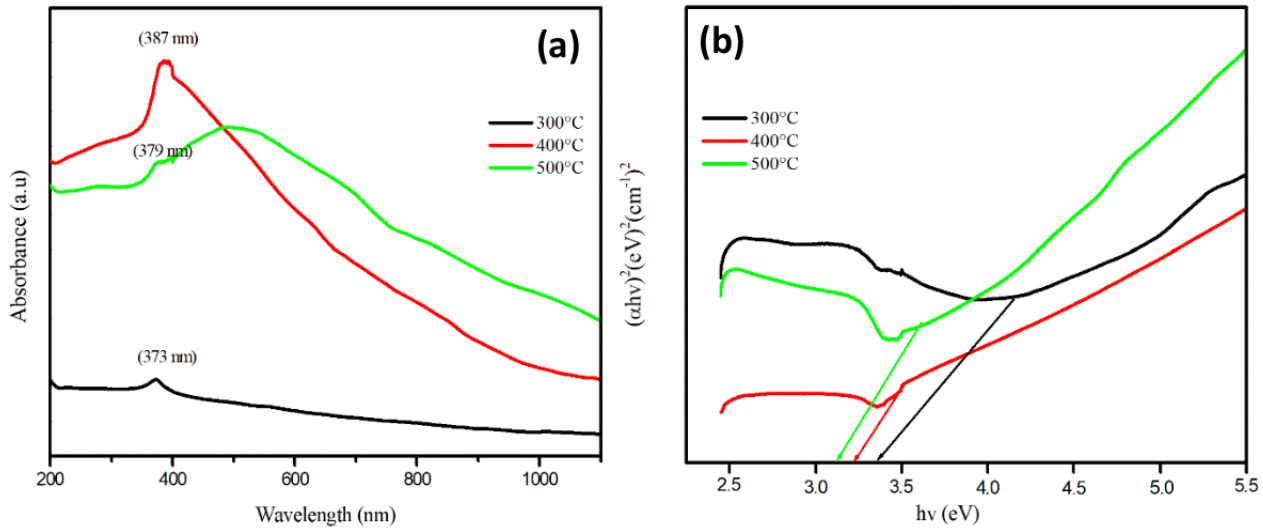

Figure 2: a) UV-Visible spectra (b) optical band gap energy of the biosynthesized ZnO nanoparticles calcined at three different temperatures

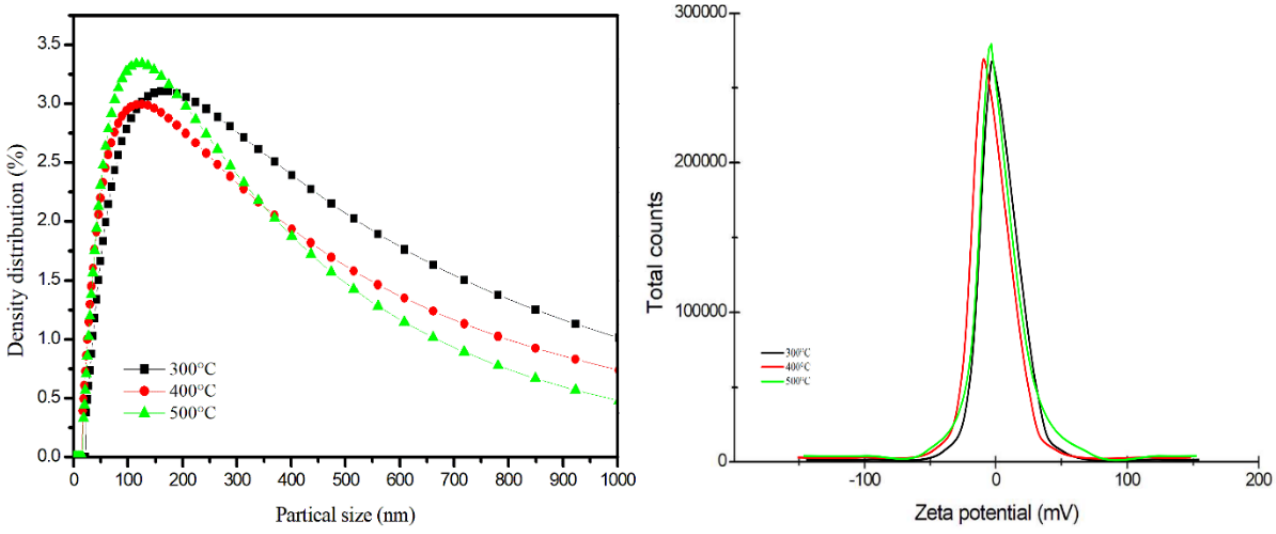

Figure 3: (a) DLS (b) Zeta potential of the biosynthesized ZnO nanoparticles calcined at three different temperatures

Table 2: EDX element value of biosynthesized ZnO nanoparticles at different calcinations temperature

ZnO NPs	Element	Weight %	Atomic %
300 °C	O K	27.9	61.2
	ZnK	72.1	38.8
400 °C	O K	21.5	52.8
	ZnL	78.5	47.2
500 °C	O K	24	56.3
	ZnL	76	43.7

of *O. sanctum* leaf extract exhibited several peaks at 3420.27, 2978.25, 2491.98, 1437.04, 859.69 and 681.52 cm^{-1}. The peaks at 3420.27 (O-H), 2978.25 (CH_2), 2491.98 (stretching mode of C-H), 1437.04 (bending mode of C-H), 800-600 (RCOO)cm^{-1} are associated to flavonoids, phenolic and alkaloids compounds correspondingly [3, 9, 18]. Functional groups analysis confirmed the incidence of carboxyl and amide groups in the *O. sanctum* leaf extract. In this process, zinc ions are transformed into ZnO nanoparticles by the groups.

Depending on the calcined temperature, the major absorption bands of synthesized nanoparticles are 3450-3350, 2950-2900, 2450-2350, 1450-1400, and 500-400 cm -1 (Figure 6). A broad fascination peak at 3450-3350 cm^{-1} is caused by stretching vibrations between O and H, which are found in phenolic and carboxylic acids [3]. An alkyl peak was observed at 2450-2350 cm^{-1} in the O-H group [29]. Assigned to N-O stretching in the nitro group, the peak at 1450-1400 cm^{-1} was strong [30]. In each samples showed an intense broad band in the range 500-400 cm^{-1} due to ZnO nanocrystals vibrational property [3, 18]. Nitrates are biotransformed into oxides by phytochemicals as a result. Biosynthesized ZnO nanoparticles showed new characteristic peaks as compared to pure ZnO nanoparticles [3]. 2974.25 and 1437.04 cm^{-1} were peaks created by flavonoids

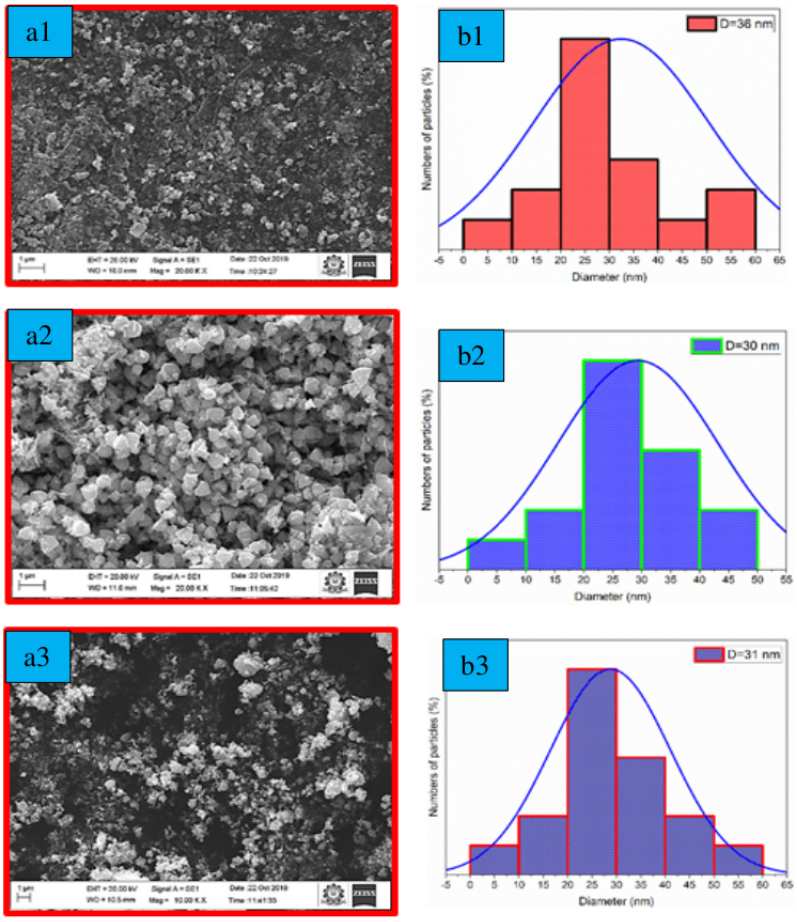

Figure 4: a1-a3) SEM and (b1-b3) particles size distribution of biosynthesized ZnO nanoparticles calcined at three different temperatures

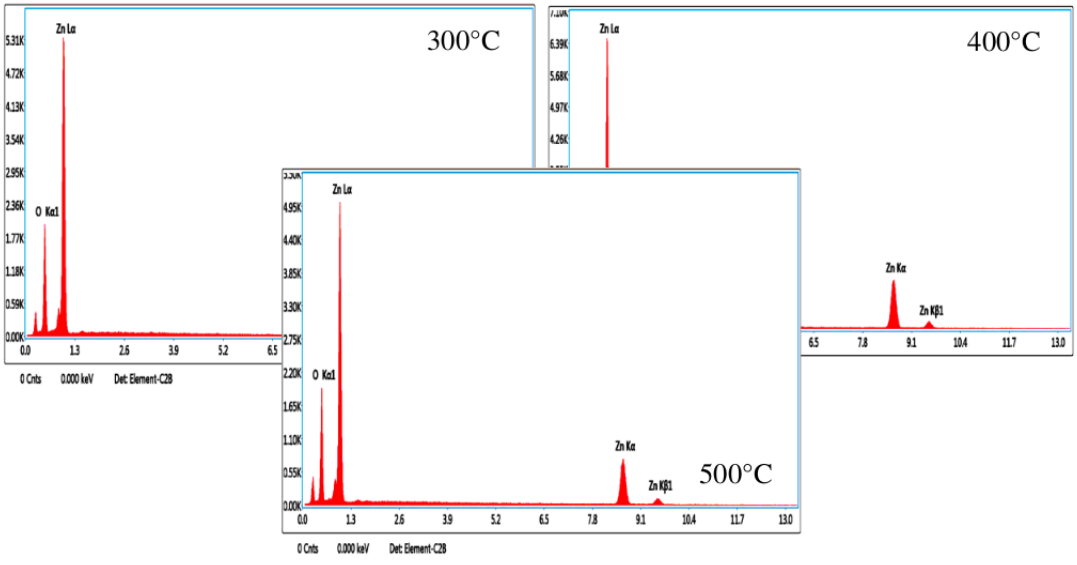

Figure 5: EDX images of ZnO nanoparticles calcined at three different temperatures

and phenolics of leaf extract molecules, confirming the presence of phytochemicals on ZnO nanoparticles. A phytochemical from plant materials acts as a reducing agent during the formation of nanoparticles.

3.6. PL analysis

Figure 7 shows a photoluminescence result of three different calcined ZnO nanoparticles in powder form excited at 320 nm at room temperature. On the absorption spectrum, Near

Table 3: Antibacterial activity of leaf extract and biosynthesized (400°C) ZnO nanoparticles against human pathogens

Bacteria	Concentrations					
	5 μg/mL			10 μg/mL		
	Leaf	Bio	Standard	Leaf	Bio	Standard
Bacillus subtilis	4	12	15	9	22	25
Staphylococcus aureus	5	10	14	10	23	25
Pseudomonas aeruginosa	5	14	16	11	24	26
Escherichia coli	7	14	17	13	25	26

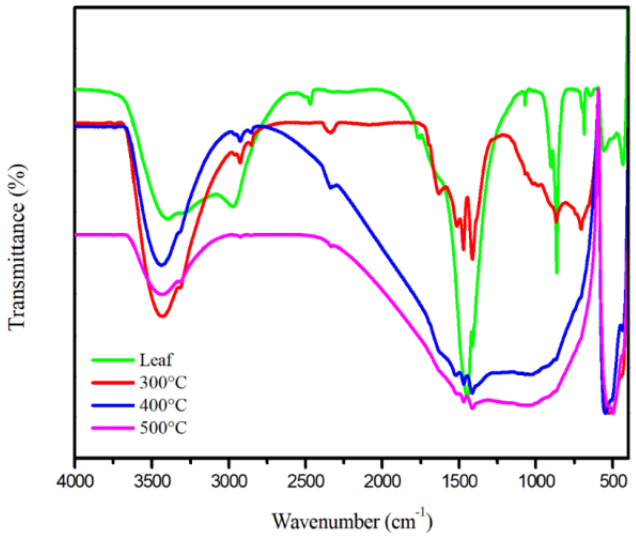

Figure 6: FT-IR spectra of the biosynthesized ZnO nanoparticles calcined at three different temperatures

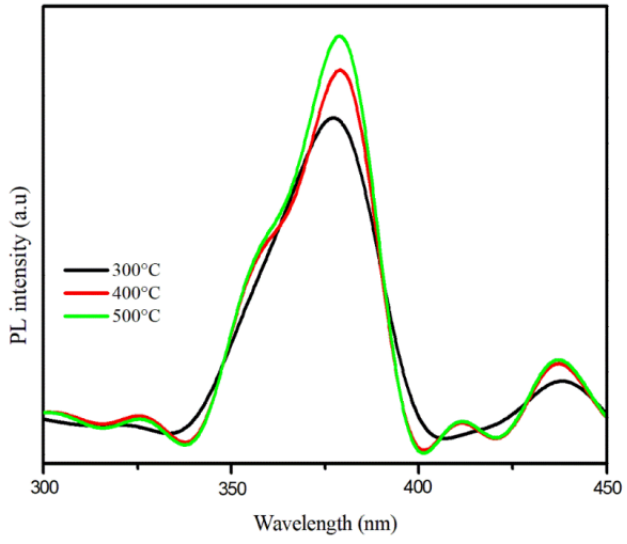

Figure 7: PL spectra of the biosynthesized ZnO nanoparticles calcined at three different temperatures

Band Edge (NBE) emission peaks at 360-370 nm are typically associated with donor band excitation emission [31]. There are in the blue region of the PL spectrum around 412 and 434 nm. through an exciton collision process, the peak at 412 nm results from the recombination of free excitons [32]. Photogenerated holes and electrons occupying oxygen vacancies are thought to generate the peak at 434 nm by radiative recombination [32]. As electron and holes recombine under light irradiation, they emit PL and the lower intensity of PL indicates a lower electron hole recombination [3]. When biosynthesized ZnO nanoparticles at 400 and 500 $^{\circ}C$ as compared 300 $^{\circ}C$, their PL intensity is highest, indicating the most electron and hole recombination [33]. The biosynthesized ZnO nanoparticles exhibit some surface and subsurface defects as a result of their dissolute response formation progression and huge surface to size ratio.

3.7. Antibacterial activities

Figure 8 shows the bacterial activity of *O. sanctum* leaf extract and biosynthesized ZnO nanoparticles (400$^{\circ}C$) were examined by both Gram-positive (*Bacillus subtilis* and *Staphylococcus aureus*) and gram-negative (Pseudomonas aeruginosa and *Escherichia coli*) bacteria by disk diffusion technique. The size of the reserve zone growths linearly with an increase in sample concentration (Table 3). In higher concentrations, leaf extract showed very little bacterial activities with zones of inhibition of the bacteria such as; *Bacillus subtilis* (9 nm), *Staphylococcus aureus* (10 nm), Pseudomonas aeruginosa (11 nm) and *Escherichia coli* (13 nm). The phytochemicals in *O. sanctum* leaf extract may be in control for the vey little antibacterial activity present in it. Based on the antibacterial activity results, biosynthesized ZnO nanoparticles were effective against all tested bacteria.

The zone of shyness was originated to be the *Escherichia coli* (25 mm), Pseudomonas aeruginosa (24 mm), *Staphylococcus aureus* (23 mm) and *Bacillus subtilis* (22 mm) at 10 μg/mL concentrations. Gram negative bacteria are more susceptible to biosynthesized ZnO nanoparticles than gram positive microbes. There was a variance in the cell wall assets of Gram positive and Gram-negative bacteria, with Gram positives having a heavier outer cell membrane layer, which made them immune to ZnO nanoparticles. In addition, it was proposed that gram negative bacteria were immune to nanoparticles due to lip polysac-

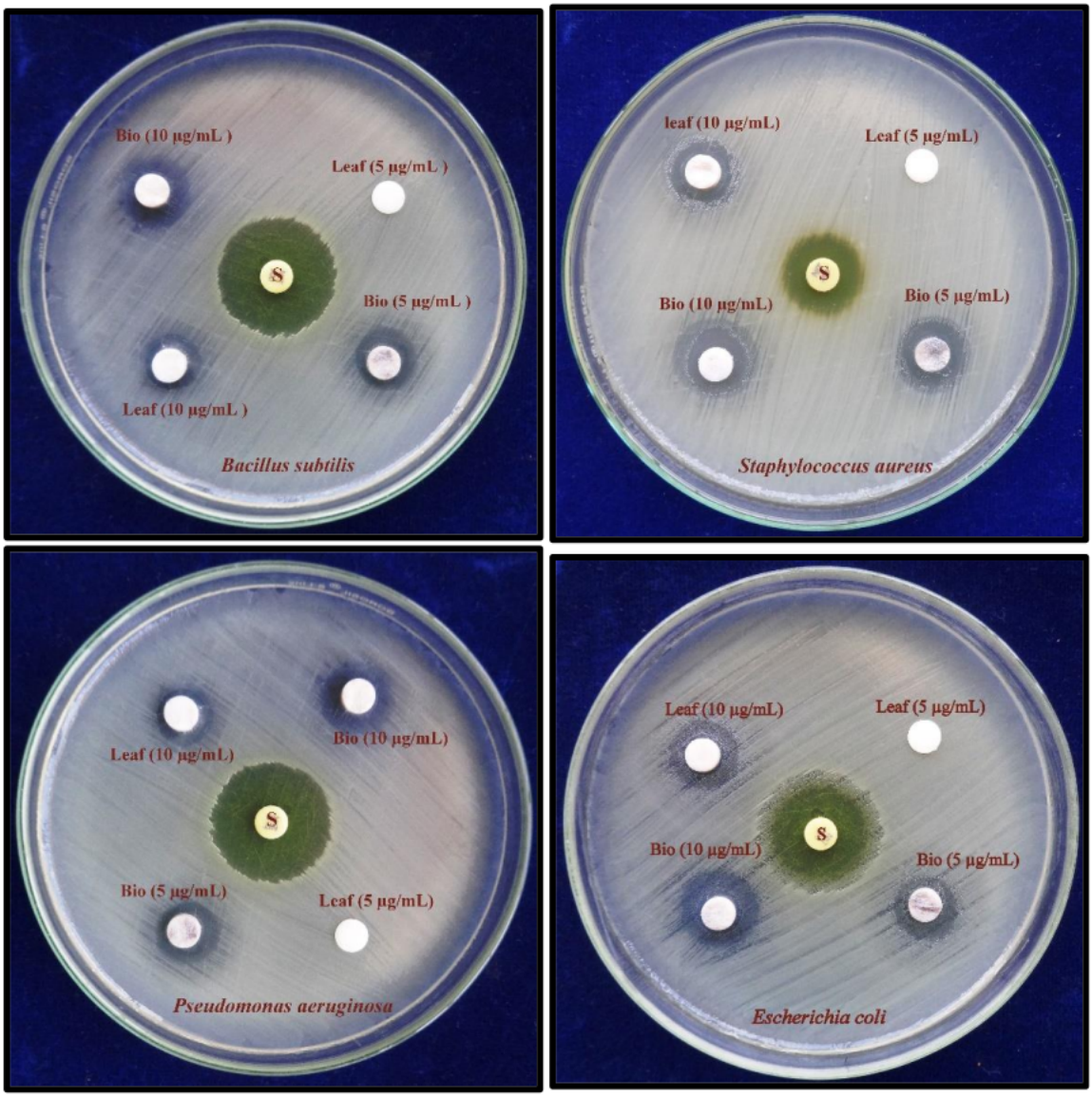

Figure 8: Antibacterial activity of the *O. sanctum* leaf extract and biosynthesized (400°*C*) ZnO nanoparticles against human pathogens

charide on their cell walls. In a statement by Muthuvel et al [3], the antibacterial activities of biosynthesized ZnO nanoparticles were stated to be additional active against gram negative bacteria than gram positive microorganisms. ZnO nanoparticles consume a variety of mechanisms for causing antibacterial action, the most common of which is the production of ROS and the statement of Zn^{2+}, which result in cell impairment and demise in bacteria [18]. Moreover, because ZnO nanoparticles are cations, they can electrostatically ascribe to the damagingly emotional surface of bacteria, instigating them to become injured. The biosynthesized ZnO nanoparticles presented greater bacterial activities in the present study because of their insignificant size and stability. Comparatively, to bulk nanoparticles, smaller nanoparticles (crystallite size 12 nm) have a higher surface range and reactivity, which improves their bacterial activity. Among the biosynthesized ZnO nanoparticles with an average size of 3 nm, Muthuvel et al [3] observed sophisticated inhibitory activity against Pseudomonas aeruginosa and *Escherichia coli* microorganisms. They also proposed that the bacterial activities of ZnO nanoparticles is size dependent, and that they inhibited *Escherichia coli* growth at a comparatively low concentration of 10 μg/mL [34].

4. Conclusion

The impact of different calcining temperature (300-500 °*C*) on the classification of the synthesized nanoparticles was examined with different techniques such as UV-vis, PL, SEM with EDAX, XRD, DLS, ZE and FT-IR. XRD results indicate that all samples are crystallized from wurtzite ZnO with good crystallinity. The SEM reveal that the ZnO nanoparticles synthesized at 400 °*C* yielded the best size and shape, while at 500 °*C*, the particles agglomerated and became large. The FT-IR results showed that biomolecules were involved in reducing

zinc ions to ZnO nanoparticles as well as acting as a capping agent for the synthesized ZnO. The ZE value was found to be -26.48 mV. The high worth indicates that zinc oxide nanoparticles are stable. The bacterial activity of the biosynthesized ZnO nanoparticles were assessed by disk diffusion technique towards all tested bacteria showed effective inhibitory activity against *Escherichia coli* (25 mm) and Pseudomonas aeruginosa (24 mm). It is a simple, eco-friendly and economically feasible way to apply and extend the green chemistry methods to nanoparticles production. There is a potential that biosynthesized nanoparticles can be used in a variety of fields, including cosmetics and pharmaceuticals.

References

[1] B. H. Abbasi, H. Fazal, N. Ahmad, M. Ali, N. Giglioli-Guivarch, & C. Hano, "Nanomaterials for cosmeceuticals: nanomaterials-induced advancement in cosmetics, challenges, and opportunities", Nanocosmetics (2020) 79.

[2] P. Thamilmaran, M. Arunachalam, S. Sankarrajan, & K. Sakthipandi, "On-line ultrasonic characterisation of barium doped lanthanum perovskites", Physica B: Condensed Matter **466** (2015) 19.

[3] A. Muthuvel, M. Jothibas, & C. Manoharan, "Effect of chemically synthesis compared to biosynthesized ZnO-NPs using *Solanum nigrum* leaf extract and their photocatalytic, antibacterial and in-vitro antioxidant activity", J. Environ. Chem. Eng. **8** (2020) 103705.

[4] A. Muthuvel, M. Jothibas, & C. Manoharan, "Synthesis of copper oxide nanoparticles by chemical and biogenic methods: photocatalytic degradation and in vitro antioxidant activity", Nanotechnol. Environ. Eng. **5** (2020) 2.

[5] A. A. Faremi, S. S. Oluyamo, K. D. Adedayo, Y. A. Odusote, & O. I. Olusola, "Influence of Silicon Nanoparticle on the Electrical Properties of Heterostructured CdTe/CdS thin films based Photovoltaic Device", Journal of the Nigerian Society of Physical Sciences (2021) 256. doi:10.46481/jnsps.2021.267

[6] A. F. Afolabi, S. S. Oluyamo, & I. A. Fuwape, "Synthetic Characterization of Cellulose from Moringa oleifera seeds and Potential Application in Water Purification", Journal of the Nigerian Society of Physical Sciences (2021). doi:10.46481/jnsps.2021.206

[7] C. Thangamani, PV Kumar, K Gurushankar, & K Pushpanathan, "Structural and size dependence magnetic properties of Mn-doped NiO nanoparticles prepared by wet chemical method", Journal of Materials Science: Materials in Electronics **31** (2020) 11101.

[8] A. Muthuvel, N. M. Said, M. Jothibas, K. Gurushankar, & V. Mohana, "Microwave- assisted green synthesis of nanoscaled titanium oxide: photocatalyst, antibacterial and antioxidant properties", J. Mater. Sci.: Mater. Electron. **32** (2021) 23522.

[9] M. Satheshkumar, B. Anand, A. Muthuvel, M. Rajarajan, V. Mohana, & A. Sundaramanickam, "Enhanced photocatalytic dye degradation and antibacterial activity of biosynthesized ZnO-NPs using *Curry* leaves extract with coconut water", Nanotechnol. Environ. Eng. **5** (2020) 3.

[10] K. Gurushankar, S. Jeyavijayan, M. Gohulkumar & K. Viswanathan, "Synthesis, Optical and Morphological Studies of ZnO Nanoparticles Capped with PVP as a Surfactant", International Journal of Chemical Sciences **16** (2018) 240.

[11] S. Y. Bae, H. W. Seo, & J. Park, "Vertically Aligned Sulfur-Doped ZnO Nanowires Synthesized via Chemical Vapor Deposition", ChemInform, 35 (2004) 30.

[12] N. Goswami & D. K. Sharma, "Structural and optical properties of unannealed and annealed ZnO nanoparticles prepared by a chemical precipitation technique", Physica E Low Dimens. Syst. Nanostruct. **42** (2010) 1675.

[13] S. Bazazi, N. Arsalani, A. Khataee, & A. G. Tabrizi, "Comparison of ball milling- hydrothermal and hydrothermal methods for synthesis of ZnO nanostructures and evaluation of their photocatalytic performance", J. Ind. Eng. Chem. **62** (2018) 265.

[14] W. Chen, C. Yao, J. Gan, K. Jiang, Z. Hu, J. Lin, N. Xu, J. Sun, & J. Wu, "ZnO colloids and ZnO nanoparticles synthesized by pulsed laser ablation of zinc powders in water", Mater Sci Semicond Process **109** (2020) 104918.

[15] D. Saravanakkumar, S. Sivaranjani, K. Kaviyarasu, A. Ayeshamariam, B. Ravikumar, S. Pandiarajan, C. Veeralakshmi, M. Jayachandran, & M. Maaza, "Synthesis and characterization of ZnO-CuO nanocomposites powder by modified perfume spray pyrolysis method and its antimicrobial investigation", J. Semicond. **39** (2018) 033001.

[16] M. Alavi & A. Nokhodchi, "Synthesis and modification of bio-derived antibacterial Ag and ZnO nanoparticles by plants, fungi, and bacteria", Drug Discov. **26** (2021) 1953.

[17] N. Al-Zaqri, A. Muthuvel, M. Jothibas, A. Alsalme, F. A. Alharthi, & V. Mohana, "Biosynthesis of zirconium oxide nanoparticles using Wrightia tinctoria leaf extract: Characterization, photocatalytic degradation and antibacterial activities", Inorg. Chem. Commun. **127** (2021) 108507.

[18] K. Elumalai & S. Velmurugan, "Green synthesis, characterization and antimicrobial activities of zinc oxide nanoparticles from the leaf extract of *Azadirachta indica* (L.)", Appl. Surf. Sci. **345** (2015) 329.

[19] J. Santhoshkumar, S. V. Kumar, & S. Rajeshkumar, "Synthesis of zinc oxide nanoparticles using plant leaf extract against urinary tract infection pathogen", Resource-Efficient Technologies **3** (2017) 459.

[20] N. Matinise, X. G. Fuku, K. Kaviyarasu, N. Mayedwa, & M. Maaza, "ZnO nanoparticles via Moringa oleifera green synthesis: Physical properties and mechanism of formation", Appl. Surf. Sci. **406** (2017) 339.

[21] M. A. Ansari, M. Murali, D. Prasad, M. A. Alzohairy, A. Almatroudi, M. N. Alomary, A. C. Udayashankar, S. B. Singh, S. M. M. Asiri, B. S. Ashwini, H. G. Gowtham, N. Kalegowda, K. N. Amruthesh, T. R. Lakshmeesha, & S. R. Niranjana, "*Cinnamomum verum* Bark Extract Mediated Green Synthesis of ZnO Nanoparticles and Their Antibacterial Potentiality", Biomolecules **10** (2020) 336.

[22] A. Chaudhary, S. Sharma, A. Mittal, S. Gupta, & A. Dua, "Phytochemical and antioxidant profiling of *Ocimum sanctum*", Journal of Food Science and Technology, **57** (2020) 3852.

[23] A. Muthuvel, K. Adavallan, K. Balamurugan, & N. Krishnakumar, "Biosynthesis of gold nanoparticles using *Solanum nigrum* leaf extract and screening their free radical scavenging and antibacterial properties", Biomed. Prev. Nutr. **4** (2014) 325.

[24] S. Vijayakumar, B. Vaseeharan, B. Malaikozhundan, & M. Shobiya, "Laurus nobilis leaf extract mediated green synthesis of ZnO nanoparticles: Characterization and biomedical applications", Biomed. Pharmacother. **84** (2016) 1213.

[25] A. Khorsand Zak, W. H. Abd. Majid, M. R. Mahmoudian, M. Darroudi, & R. Yousefi, "Starch-stabilized synthesis of ZnO nanopowders at low temperature and optical properties study", Adv Powder Technol. **24** (2013) 618.

[26] V. Ramasamy, V. Mohana, & V. Rajendran, "Characterization of Ca doped CeO2 quantum dots and their applications in photocatalytic degradation", OpenNano. **3** (2018) 38.

[27] A. M. Ismail, A. A. Menazea, H. A. Kabary, A. E. El-Sherbiny, & A. Samy, "The influence of calcination temperature on structural and antimicrobial characteristics of zinc oxide nanoparticles synthesized by Sol-Gel method", J. Mol. Struct. **1196** (2019) 332.

[28] J. Emegha, B. Olofinjana, K. Ukhurebor, U. Aigbe, S. Azi, & M. Eleruja, "Effect of Deposition Temperature on the Properties of Copper-Zinc Sulphide Thin Films using Mixed Copper and Zinc Dithiocarbamate Precursors", Gazi University Journal of Science, Nov. 2021.

[29] P. A. Arciniegas-Grijalba, M. C. Patino-Portela, L. P. Mosquera-Sánchez, J. A. Guerrero-Vargas, & J. E. Rodriguez-Paez, "ZnO nanoparticles (ZnO-NPs) and their antifungal activity against coffee fungus Erythricium salmonicolor", Appl. Nanosci. **7** (2017) 225.

[30] A. Abioye, M. Naqvi, D. Pattni, & A. A. Adepoju-Bello, "Non-intuitive Behavior of Polymer-Ciprofloxacin Nanoconjugate Suspensions: a Tool for Flexible Oral Drug Delivery", AAPS Pharm. Sci. Tech. **22** (2021) 7.

[31] K. Velsankar, S. Sudhahar, G. Parvathy, & R. Kaliammal, "Effect of cytotoxicity and aAntibacterial activity of biosynthesis of ZnO hexagonal shaped nanoparticles by Echinochloa frumentacea grains extract as a reducing agent", Mater. Chem. Phys. **239** (2020) 121976.

[32] U. Wijesinghe, G. Thiripuranathar, H. Iqbal, & F. Menaa, "Biomimetic Synthesis, Characterization, and Evaluation of Fluorescence Resonance Energy Transfer, Photoluminescence, and Photocatalytic Activity of Zinc Oxide Nanoparticles", Sustainability **13** (2021) 2004.

[33] F. Deschler, M. Price, S. Pathak, L. E. Klintberg, D.-D. Jarausch, R.

Higler, S. Hüttner, T. Leijtens, S. D. Stranks, H. J. Snaith, M. Atatüre, R. T. Phillips, & R. H. Friend, "High Photoluminescence Efficiency and Optically Pumped Lasing in Solution-Processed Mixed Halide Perovskite Semiconductors", J. Phys. Chem. Lett. **5** (2014) 1421.

[34] B. Lallo da Silva, B. L. Caetano, B. G. Chiari-Andréo, R. C. L. R. Pietro, & L. A. Chiavacci, "Increased antibacterial activity of ZnO nanoparticles: Influence of size and surface modification", Colloids Surf. B: Biointerfaces **177** (2019) 440.